



# Activation-Dependent TRAF3 Exon 8 Alternative Splicing Is Controlled by CELF2 and hnRNP C Binding to an Upstream Intronic Element

Astrid-Solveig Schultz,<sup>a</sup> Marco Preussner,<sup>a</sup> Mario Bunse,<sup>b</sup> Rotem Karni,<sup>c</sup> Florian Heyd<sup>a</sup>

Freie Universität Berlin, Institute of Chemistry and Biochemistry, Berlin, Germany<sup>a</sup>; Max Delbrück Center for Molecular Medicine, Berlin, Germany<sup>b</sup>; Department of Biochemistry and Molecular Biology, Institute for Medical Research Israel-Canada, Hebrew University-Hadassah Medical School, Ein Karem, Jerusalem, Israel<sup>c</sup>

**ABSTRACT** Cell-type-specific and inducible alternative splicing has a fundamental impact on regulating gene expression and cellular function in a variety of settings, including activation and differentiation. We have recently shown that activation-induced skipping of TRAF3 exon 8 activates noncanonical NF- $\kappa$ B signaling upon T cell stimulation, but the regulatory basis for this splicing event remains unknown. Here we identify *cis*- and *trans*-regulatory elements rendering this splicing switch activation dependent and cell type specific. The *cis*-acting element is located 340 to 440 nucleotides upstream of the regulated exon and acts in a distance-dependent manner, since altering the location reduces its activity. A small interfering RNA screen, followed by cross-link immunoprecipitation and mutational analyses, identified CELF2 and hnRNP C as *trans*-acting factors that directly bind the regulatory sequence and together mediate increased exon skipping in activated T cells. CELF2 expression levels correlate with TRAF3 exon skipping in several model systems, suggesting that CELF2 is the decisive factor, with hnRNP C being necessary but not sufficient. These data suggest an interplay between CELF2 and hnRNP C as the mechanistic basis for activation-dependent alternative splicing of TRAF3 exon 8 and additional exons and uncover an intronic splicing silencer whose full activity depends on the precise location more than 300 nucleotides upstream of the regulated exon.

**KEYWORDS** RNA binding proteins, RNA splicing

Splicing-sensitive microarrays and transcriptome sequencing (RNA-Seq) technologies have led to the accumulation of enormous amounts of gene expression data from different cell types and tissues under various conditions. Such analyses have led to the conclusion that the majority of human genes are alternatively spliced and have shown strong differences in global splicing patterns under different conditions (1–3). Although these differences suggest a substantial contribution of alternative splicing to the regulation of gene expression, studies connecting alternative splicing and functionality are rare. Consequently, a functional impact of individual alternative splicing events on cellular functionality was demonstrated for only a few examples (4–7), and the function of most alternative splicing events remains unknown. However, a recent large-scale approach demonstrated that splice-isoforms of the same gene often have distinct protein-protein interaction profiles, further supporting the notion of distinct functionality (8).

Another largely open question concerns splicing regulation: how are cell-type-specific splicing patterns established and maintained? Despite the identification of

Received 5 September 2016 Returned for modification 27 September 2016 Accepted 20 December 2016

Accepted manuscript posted online 28 December 2016

**Citation** Schultz AS, Preussner M, Bunse M, Karni R, Heyd F. 2017. Activation-dependent TRAF3 exon 8 alternative splicing is controlled by CELF2 and hnRNP C binding to an upstream intronic element. *Mol Cell Biol* 37:e00488-16. <https://doi.org/10.1128/MCB.00488-16>.

**Copyright** © 2017 American Society for Microbiology. All Rights Reserved.

Address correspondence to Florian Heyd, [florian.heyd@fu-berlin.de](mailto:florian.heyd@fu-berlin.de).

some splicing factors that are preferentially or exclusively expressed in a certain cellular context, e.g., CELF1/MBNL1, NOVA, nPTB, ESRP1/2, or U2AF26 (9–13), mechanisms that control cell-type-specific alternative splicing remain to be discovered in many cases. The decision whether or not an alternative exon is included in the mature mRNA depends on (i) *cis*-regulatory RNA elements and (ii) binding of *trans*-acting factors that control spliceosome recruitment and ultimately splicing (14). Although some splice events are known where one splicing factor is the dominant regulator, in many cases alternative splicing is determined by the sum of the activity of several splicing regulatory proteins (15, 16). The activity of such proteins can be controlled by changes in expression or by posttranslational modifications that can control localization or RNA binding capability for example (17–21). Altered activity may then result in alternative splicing of several or many exons in a concerted manner, thus contributing to establish global splicing patterns, for example in a tissue-specific manner (9, 22–25).

CELF2 is an RNA-binding protein that is expressed in a tissue-specific manner, e.g., during embryonic development and heart formation (26, 27). CELF2 controls a variety of alternative exons with functional implications for differentiation and functionality of the respective tissues (28). CELF2 expression is also increased upon differentiation of primary human thymocytes and activation of a model T cell line (Jsl1), where it regulates alternative splicing of the transcription factor Lef1 and other targets (29, 30).

We have recently shown that exclusion of TRAF3 exon 8 is increased upon T cell activation and induces  $\kappa$ B signaling to control chemokine expression (31). This induction is based on differential interaction of the two TRAF3 isoforms with the kinase NIK, which, upon activation-induced exclusion of TRAF3 exon 8, is released from a ubiquitin-ligase complex. Formation of this complex in unstimulated T cells leads to constant NIK degradation and low basal NIK expression. NIK can therefore only accumulate in activated, TRAF3 $\Delta$ E8-expressing T cells, where it triggers the activation of  $\kappa$ B signaling (31). In the present work, we have identified the mechanistic basis for activation-dependent and cell-type-specific TRAF3 exon 8 skipping. We show that CELF2 and hnRNP C, a protein that has, for example, been implicated in preventing the exonization of Alu elements (32), bind a U-rich intronic splicing silencer (ISS) 340 to 440 nucleotides (nt) upstream of TRAF3 exon 8. This leads to activation-induced exon skipping, which, in minigenes, is dependent on the distance of the splicing silencer to the regulated exon. Although the binding of both proteins CELF2 and hnRNP C is required for exon skipping, neither protein alone is sufficient. Since the activity of this intronic splicing silencer correlates with the abundance of CELF2 protein, we suggest that the CELF2 expression is the main determinant of cell-type-specific and activation-induced alternative splicing of TRAF3 exon 8 and coregulated exons. hnRNP C, in contrast, appears to be necessary but is neither sufficient nor limiting for TRAF3 exon 8 exclusion, since its expression alone does not lead to exon exclusion. Furthermore, our data define an intronic *cis*-regulatory element located outside the 300-nt boundary of intronic sequence frequently used to analyze splicing regulation and may lead to the discovery of more exons regulated through such distantly localized regulatory sequences in future studies.

## RESULTS

**An intronic splicing silencer regulates activation-induced TRAF3 exon 8 skipping.** To gain mechanistic insight into activation-induced TRAF3 exon 8 skipping, we characterized *cis*-acting RNA sequences in a minigene approach. We used a vector containing constitutive CD45 exons as flanking exons (33) and first cloned a minigene (designated minigene 1) containing ~6 kb of TRAF3 genomic sequence comprising exons 7 to 9. This construct fully mimics activation-induced splicing regulation when transfected into Jsl1 T cells (Fig. 1A and B). A construct containing only the alternative exon 8 and ~1.2 kb of the upstream and 1.3 kb of the downstream intron (minigene 2) showed a similar responsiveness to phorbol myristate acetate (PMA) stimulation. In contrast, a minigene containing only exon 8 and ca. 300 bp (upstream) or 400 bp (downstream) of the surrounding introns showed no activation-induced exon skipping

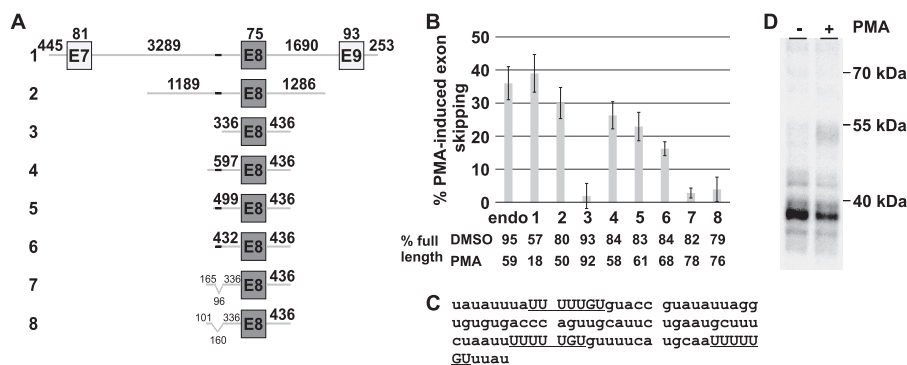


**FIG 1** Identification of *cis*-acting element that mediates TRAF3 exon 8 alternative splicing. (A) Schematic presentation of TRAF3 exon-intron structure around exons 7 to 9 and minigene constructs. Exons are indicated by boxes (not to scale), and introns are indicated by lines. The length of the exonic or intronic sequence in bp is indicated above the respective fragment. For constructs 7 and 8, the number below the scheme indicates deleted base pairs. The *cis*-acting intronic element is shown in boldface. (B) Jsl1 cells were transfected with the minigene variants shown in panel A and treated with DMSO or PMA for 48 h. Splicing of the transfected TRAF3 minigenes was analyzed by radioactive RT-PCR and quantified by phosphorimager analysis. Endogenous TRAF3 splicing is shown in the first bar. Values are mean values from at least three different experiments with standard deviation. Mean values of the percentages of full-length product in unstimulated (DMSO) or stimulated (PMA) cells are shown below the graph. (C) Sequence of the *cis*-acting element for TRAF3 exon 8 splicing identified in panel B. A sequence motif that occurs three times is underlined. (D) UV cross-link with the RNA shown in panel C with nuclear extracts from resting (–) or stimulated (+) Jsl1 cells.

(minigene 3), suggesting that intronic sequences outside these boundaries are required for splicing regulation (Fig. 1A and B). Increasing the length of this construct identified an intronic element upstream of the regulated exon, which led to PMA-induced exon skipping (construct 4 in Fig. 1A and B). This splicing change is only slightly smaller than the one observed in minigene 2 (that contains larger intronic regions on either site of the exon), suggesting that construct 4 contains the main *cis*-regulatory sequence. Successively shortening the upstream intronic sequence in construct 4 slightly reduced the PMA responsiveness (construct 4 versus constructs 5 and 6), but a minigene containing only 96 nt of the regulatory sequence (construct 6) still showed substantial activation-induced exon skipping. Deletion of these 96 nt in the context of the surrounding intron led to an almost complete loss of PMA responsiveness (construct 7), as did deletion of a larger part of the regulatory element (construct 8). We thus conclude that the 96 bp deleted in construct 7 represent the core *cis*-regulatory element, since their deletion is sufficient to abrogate PMA-induced exon skipping (compare constructs 4 and 7). Of note, minigene 4 displays a slightly reduced PMA-responsiveness compared to the endogenous TRAF3 exon 8, pointing to the contribution of additional *cis*-regulatory elements. First analyses indicate the presence of an element downstream of TRAF3 exon 8 that acts independently to contribute to the regulation in the endogenous situation (data not shown). In the present work we focused on the upstream 96 nt identified in Fig. 1A and B, since our data suggest this sequence to contain the main PMA-responsive element. A noticeable feature of this sequence are three stretches of five or more U's followed by GU (Fig. 1C, underlined).

Having identified a *cis*-acting element that is necessary for activation-induced exon skipping, we went on to characterize *trans*-acting factors binding to this RNA sequence. In a first approach, we used a UV cross-link assay with radiolabeled RNA. These experiments identified several proteins directly binding to the *cis*-acting element. A protein with an apparent size of just under 55 kDa caught our attention, since it shows strongly increased binding to the *cis*-acting sequence in PMA-stimulated T cells (Fig. 1D).

**An siRNA screen identifies CELF2 to mediate TRAF3 exon 8 exclusion in activated T cells.** To identify the 55-kDa protein, which was found to bind the *cis*-regulatory sequence upon stimulation in the UV cross-link experiment (Fig. 1D), a targeted small interfering RNA (siRNA) screen was performed. We transfected Jsl1 T cells with ~100

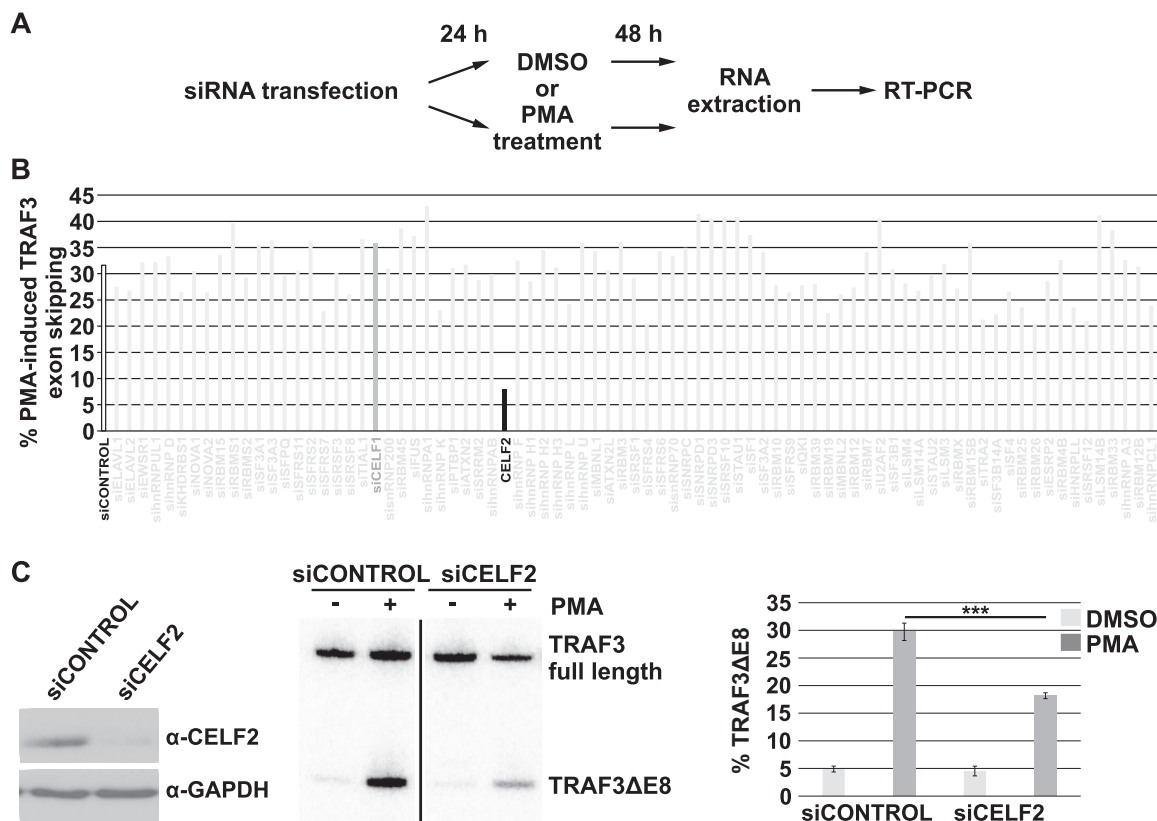


**FIG 2** An siRNA screen identifies CELF2 as *trans*-acting factor in TRAF3 exon 8 splicing. (A) Scheme showing the screening strategy. Jsl1 cells were transfected with siRNA and divided 24 h later to treat them with DMSO or PMA. Cells were harvested at 48 h poststimulation. TRAF3 exon 8 splicing was analyzed by RT-PCR and quantified by phosphorimager analysis. (B) Jsl1 cells were transfected with approximately 100 siRNAs pools (consisting of four individual siRNAs targeting the same gene) and analyzed as described in panel A. Highlighting is used to indicate CELF2, whose knockdown has the strongest impact on TRAF3 splicing (black), and CELF1, which belongs to the same protein family but did not show any effect (dark gray). Only siRNA pools that gave consistent results in two independent RT-PCRs are shown. (C) siRNAs were transfected in Jsl1 T cells as indicated. Knockdown of CELF2 was confirmed by Western blotting (left). The effect on TRAF3 exon 8 skipping was analyzed by radioactive RT-PCR (middle) and quantified by phosphorimager analysis (right,  $n = 4$ ).

different siRNAs (pools of four siRNAs per target) against RNA-binding proteins and prepared RNAs from resting and stimulated conditions. These RNAs were then used in splicing-sensitive reverse transcription-PCRs (RT-PCRs) to assay TRAF3 exon 8 skipping (see scheme in Fig. 2A). We hypothesized that binding of the 55-kDa protein induces exon skipping in activated T cells, and its knockdown in stimulated cells is then expected to reduce PMA responsiveness. RT-PCR analyses were performed in duplicates, and only if results were consistent between the two experiments were they considered further. A summary of the screening results is presented in Fig. 2B. Almost all siRNA-transfected cells showed an increase in exon exclusion of ~30% upon stimulation, which corresponds to the effect in untransfected cells and cells transfected with a control siRNA. However, an siRNA pool directed against the mRNA of the RNA binding protein CELF2 strongly reduced PMA responsiveness (Fig. 2B). Knocking down the related protein CELF1 had no effect (Fig. 2B), confirming the specificity of the result. The effect of CELF2 knockdown on TRAF3 exon 8 skipping was validated in independently transfected cells that were also used to confirm knockdown of CELF2 protein (Fig. 2C). In this experiment, the effect on TRAF3 splicing was slightly less strong than in the initial screen, which was likely due to altered transfection conditions. Furthermore, we transfected three CELF2 siRNAs individually and measured knockdown of CELF2 mRNA and the effect on PMA-induced TRAF3 exon 8 skipping. All three siRNAs led to a substantial CELF2 knockdown and reduced PMA-induced TRAF3 exon 8 skipping (see Fig. S1 in the supplemental material). These data confirm that CELF2 is

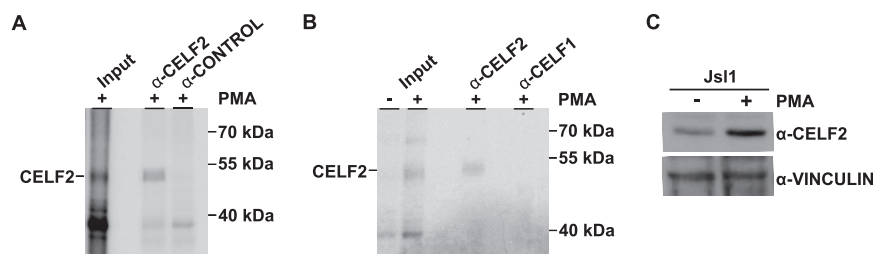


**FIG 3** CELF2 directly binds to the TRAF3 *cis*-acting element. (A and B) UV cross-links as in Fig. 1D with an IP step added. Immunoprecipitations were performed with the indicated antibodies. Representative blots from at least three independent experiments are shown. As a control, mouse anti-HA was used. (C) Western blot showing CELF2 expression in unstimulated and stimulated Jsl1 cells. Antivinculin was used as a loading control. One representative blot from at least three independent experiments is shown.

necessary for full TRAF3 exon 8 skipping upon T cell activation and are consistent with a recent RNA-Seq approach that identified TRAF3 exon 8 as a potential CELF2 target upon overexpression in mouse heart (28) (see Discussion). However, knockdown of CELF2 did not fully abolish PMA-induced TRAF3 exon 8 skipping. This suggests that other proteins contribute to the effect, which is consistent with several other siRNAs in our screen slightly reducing PMA responsiveness.

**CELF2 directly binds the TRAF3 exon 8 *cis*-regulatory sequence in activated T cells.** Interestingly, CELF2 is a protein of ~55 kDa, which corresponds to the size of the protein we had identified in our cross-link assays to bind the TRAF3 *cis*-acting RNA element preferentially upon stimulation (Fig. 1D). To bring together these observations, we performed a UV cross-link immunoprecipitation (IP) analysis with an antibody against CELF2. The protein that shows increased binding to the *cis*-acting element upon PMA stimulation can be specifically precipitated with a CELF2 antibody but not with a control antibody (antihemagglutinin [anti-HA]) (Fig. 3A). In addition, an antibody against CELF1 did not precipitate the 55-kDa protein, further confirming the specificity of the assays and the identity of the protein (Fig. 3A and B). Consistent with previous observations (29, 30), we found CELF2 expression to be increased upon T cell activation (Fig. 3C) providing a possible explanation for increased binding in our cross-link assays. Together, these experiments confirm that CELF2 inducibly binds the *cis*-acting element upstream of TRAF3 exon 8 and that this is necessary for activation-induced TRAF3 exon 8 skipping.

**CELF2 expression is regulated in a cell-type-specific manner, and its expression is sufficient for TRAF3 exon 8 exclusion in different cellular backgrounds.** In the data presented so far, we have shown that CELF2 expression is necessary for TRAF3 exon 8 exclusion upon T cell activation. However, these data did not address the question whether CELF2 expression alone is sufficient to regulate alternative splicing or if this requires additional signals, e.g., posttranslational modifications in activated T cells. To this end, we turned to two human B cell lines, Raji and Ramos, that we have previously shown to be unresponsive to PMA treatment with respect to TRAF3 alternative splicing (31) (Fig. 4A). Interestingly, when analyzed by Western blotting, these B cell lines did not show substantial amounts of CELF2 protein in resting or in PMA-stimulated conditions (Fig. 4B). We observed a small amount of a faster-migrating protein species, which may represent a smaller CELF2 isoform generated by alternative splicing of CELF2 itself. This observation suggests not only that CELF2 expression regulates activation-dependent TRAF3 alternative splicing but also that the level of CELF2 expression and its inducibility in different cell types render this splicing switch cell type specific.

The absence of endogenous CELF2 expression in Ramos and Raji cells provided an interesting model system to investigate whether CELF2 expression is sufficient to regulate TRAF3 alternative splicing or whether additional signals are required. We used a pEF vector, with a promoter that shows constant expression in resting and activated cells, and generated Ramos cells stably overexpressing CELF2 (Fig. 4C). As a control, we

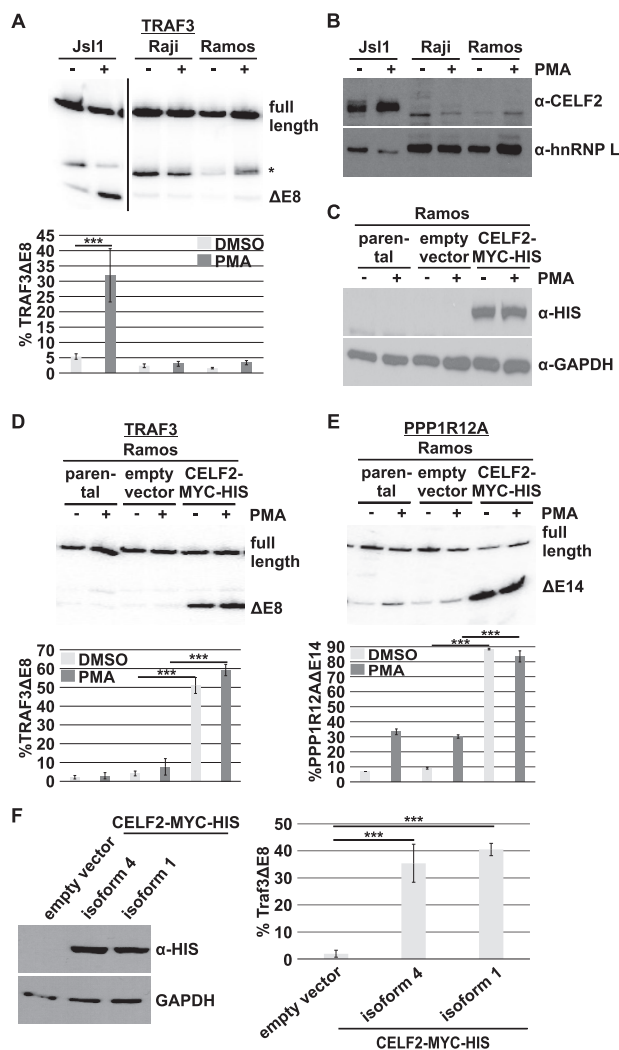


**FIG 4** CELF2 expression induces TRAF3 exon 8 skipping in different cellular backgrounds. (A) RT-PCR and quantification with RNAs from resting or activated (–/+ PMA, 48 h) Raji and Ramos B cells or Jsl1 T cells. An asterisk marks a nonspecific band comigrating with the loading dye. Values are means of at least five independent experiments. Error bars indicate standard deviations (\*\*\*,  $P < 0.001$ ). (B) Western blot of cell lysates from Jsl1, Raji, and Ramos cells (treated as in panel A). hnRNP L served as a loading control. (C) Lysates of different stable Ramos cell lines, in the presence or absence of PMA (48 h), were used for Western blot analysis with the indicated antibodies. (D and E) RT-PCR with RNAs from the different Ramos cell lines treated as in panel A. The top panel shows representative radioactive PAGE results. Below is a quantification of at least four independent stimulations (\*\*,  $P < 0.01$ ; \*\*\*,  $P < 0.001$ ). (D) TRAF3 exon 8 alternative splicing. (E) Alternative exon in PPP1R12A. (F) HEK293 cells were transfected with plasmids for the overexpression of different CELF2 isoforms. Western blotting confirming the overexpression is shown on the left. The effect on TRAF3 exon 8 alternative splicing was determined as in panel A, and the results are shown on the right. Mean values of at least three different experiments are shown.

used the parental cell line or cells that went through the same selection procedure but did not show CELF2 expression. CELF2 expression was only detectable in the overexpressing cell line and not in the two controls and did not substantially differ between resting and activated conditions (Fig. 4C). Ramos cells overexpressing CELF2 showed a dramatic increase in TRAF3 exon 8 skipping that was comparable in resting and activated cells (Fig. 4D). These data confirm the ability of CELF2 to induce TRAF3 exon 8 skipping regardless of the activation status of the cell and show that this regulation is active in different cellular backgrounds.

CELF2 has been suggested to regulate alternative splicing of many targets during T cell activation (30). We therefore investigated whether expression of CELF2 in Ramos B cells is sufficient to regulate splicing of additional exons. We chose additional targets



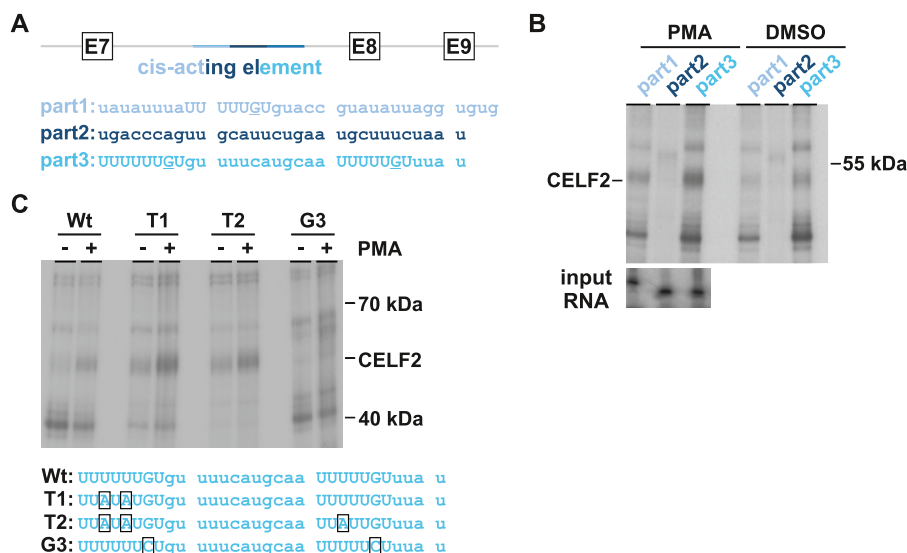


**FIG 5** Mapping CELF2 binding sites within the *cis*-regulatory element. (A) The 96-nt *cis*-acting element was divided into three parts for further experiments, as indicated. The UUUUUGU motifs in sequence part 1 and 3 are indicated by capital letters. (B) The three sequence parts shown in panel A were radioactively labeled for UV cross-link experiments with nuclear extracts from untreated (–PMA) and stimulated (+PMA) Js11 cells. A representative gel is shown. (C) Sequence part 3 and different mutations (bottom) were used for experiments as in panel B. Mutated nucleotides are indicated by boxes.

that have been described to be responsive to T cell activation and/or CELF2 knock-down, namely, PPP1R12A, BRD8, FAM36, and REPS1 (30, 34). PPP1R12A showed strongly increased exon exclusion in the CELF2-overexpressing cells, whereas the other targets showed a consistent but weaker response to CELF2 expression (Fig. 4E; see also Fig. S2 in the supplemental material). In contrast to TRAF3, PPP1R12A and BRD8 showed slight PMA-induced exon skipping in the parental and control cells that was not present in CELF2-overexpressing cells (Fig. 4E; see Fig. S2 in the supplemental material). A residual CELF2 induction in stimulated Ramos cells might be sufficient to increase exon skipping to a certain degree, and this effect could be masked in cells expressing higher levels of ectopic CELF2. Since several splicing targets showed increased exclusion in the CELF2-overexpressing Ramos cells, CELF2 expression appears to control a concerted switch in alternative splicing independent of the activation state and in different cellular backgrounds. Consistent with this model, overexpression of two different CELF2 isoforms in HEK293 cells led to strong TRAF3 exon 8 exclusion (Fig. 4F; see also Fig. 6 and Discussion).

**G residues in the intronic sequence are crucial for CELF2 binding.** Having identified CELF2 to be necessary and sufficient for TRAF3 exon 8 alternative splicing, we aimed to further characterize its interaction with the *cis*-regulatory sequence and a potential involvement of other *trans*-acting factors. To this end, we further narrowed down CELF2 binding sites within the *cis*-regulatory element by dividing the 96 nt into three parts comprising 34 (RNA1), 31 (RNA2), and 31 (RNA3) nt, respectively (Fig. 5A). We used the corresponding radiolabeled RNAs in UV cross-link assays with resting and stimulated extracts as before. RNA2 did not show any CELF2 binding (Fig. 5B); in fact, we observed very little protein binding at all to this RNA. In contrast, RNA3 and, to a lesser degree, RNA1 showed CELF2 binding that increased upon PMA stimulation (Fig. 5B). Binding patterns to RNAs 1 and 3 were very similar, although stronger in RNA3, suggesting that a common motif in both sequences mediates the majority of RNA-protein contacts. A noticeable feature in RNA3 are two stretches of five or more U residues (Fig. 1C and 5A). In a first attempt to narrow down the binding site of CELF2 within RNA3, we disrupted these U stretches by introducing U-to-A mutations. However, these mutations did not abolish but rather increased CELF2 binding (Fig. 5C, mutants T1 and T2). We then mutated the G residues following the U stretches. This

mutant almost completely lost the ability to bind CELF2, demonstrating that these residues are crucial for the interaction of CELF2 with the *cis*-acting RNA element that controls TRAF3 exon 8 alternative splicing (Fig. 5C, mutant G3). A similar motif, a U stretch followed by GU, is present in the first part of the *cis*-acting element (RNA1 [Fig. 5A, capital letters, G underlined]). The weaker binding of CELF2 and other interacting proteins to RNA1 compared to RNA3 may be due to the presence of two such sequence elements in RNA3 and only one corresponding sequence in RNA1.

**hnRNP C binds to oligo(U) stretches in the TRAF3 exon 8 *cis*-regulatory element.** Concomitant with increased CELF2 binding in the U-to-A mutants, we noticed reduced binding of a protein of ~40 kDa, which was the main band in our initial cross-link analysis (Fig. 1D). Binding of this protein was strongly reduced or lost in the U-to-A mutants (Fig. 5C). Tia1 and hnRNP C are known oligo(U)-binding protein of ~40 kDa. We therefore performed a cross-link IP with Tia1 and hnRNP C antibodies. Although we did not observe strong binding of Tia1 to the wild-type RNA (and no effect of Tia1 knockdown on TRAF3 alternative splicing [data not shown]), this experiment confirmed hnRNP C binding to the U-stretches in the TRAF3 exon 8 *cis*-regulatory sequence (Fig. 6A). Binding of hnRNP C to the U-to-A mutants was basically undetectable in the input and in cross-link IPs (Fig. 6A), confirming strongly reduced binding to these RNAs. Although we cannot formally rule out other proteins of the exact same size to cobind, it seems reasonable to assume that hnRNP C is a major component of the 40-kDa band. Interestingly, hnRNP C has been previously observed to be present on another CELF2-regulated exon (35), indicating that cobinding of both proteins on CELF2 target exons may represent a more general theme (see Discussion).

**The activity of the TRAF3 *cis*-acting sequence is dependent on binding of CELF2, hnRNP C, and the distance to the exon.** Having identified nucleotides that mediate direct contact of CELF2 and hnRNP C with the *cis*-acting element, we investigated the impact of binding of these proteins on splicing regulation. Using the mutants described above, we were able to separate hnRNP C and CELF2 binding and thus test the impact of both proteins on TRAF3 exon 8 splicing individually. We first mutated G residues crucial for CELF2 binding in all three UUUUGU motifs present in the 96-nt *cis*-regulatory sequence (Fig. 6B, construct 9; also Fig. 5A, underlined). A minigene containing these mutations basically lost PMA responsiveness (Fig. 6B), confirming that CELF2 binding to these motifs is necessary for activation-induced TRAF3 exon 8 skipping. To further analyze a role of hnRNP C binding in splicing regulation, we cloned U-to-A mutants that disrupt the interaction of hnRNP C with the RNA in our minigene (minigenes 10 and 11 [Fig. 6A and B]). These minigenes also lost PMA responsiveness (Fig. 6B), suggesting that, in addition to CELF2, hnRNP C binding is required for TRAF3 exon 8 exclusion in activated T cells. Interestingly, the expression of hnRNP C is reduced in activated T cells, whereas CELF2 expression is increased and knockdown of CELF2 does not alter hnRNP C levels (Fig. 6C). We therefore conclude that hnRNP C binding alone is not sufficient for exon exclusion (otherwise, the exon would already be excluded in resting cells) but that its binding is strictly required for the CELF2-mediated exon exclusion observed in activated T cells. This model is further supported by the finding that hnRNP C is expressed at similar levels in Jsl1, Ramos, and Raji cells (Fig. 6D), which is not sufficient to induce TRAF3 exon 8 skipping, and that the exon is only excluded upon addition of CELF2, either during T cell activation or ectopic expression in B cells or HEK293 cells. To further investigate the role of hnRNP C in TRAF3 exon skipping, we sought to reduce hnRNP C expression using siRNAs. However, we were unable to achieve efficient knockdown, especially in stimulated T cells that already show reduced hnRNP C expression. This suggests that a certain amount of hnRNP C is required for cell viability and prevented us from further testing the influence of hnRNP C in this system. We therefore turned to HEK293 cells that upon CELF2 expression show strong TRAF3 exon 8 exclusion (Fig. 4F). In these cells, we obtained reasonable hnRNP C knockdown (Fig. 6E) using siRNAs and, to make *trans*-acting factors limiting, analyzed alternative splicing of cotransfected minigene 4. In this system, knockdown of hnRNP C led to a slight but significantly reduced CELF2-mediated exon skipping, confirming



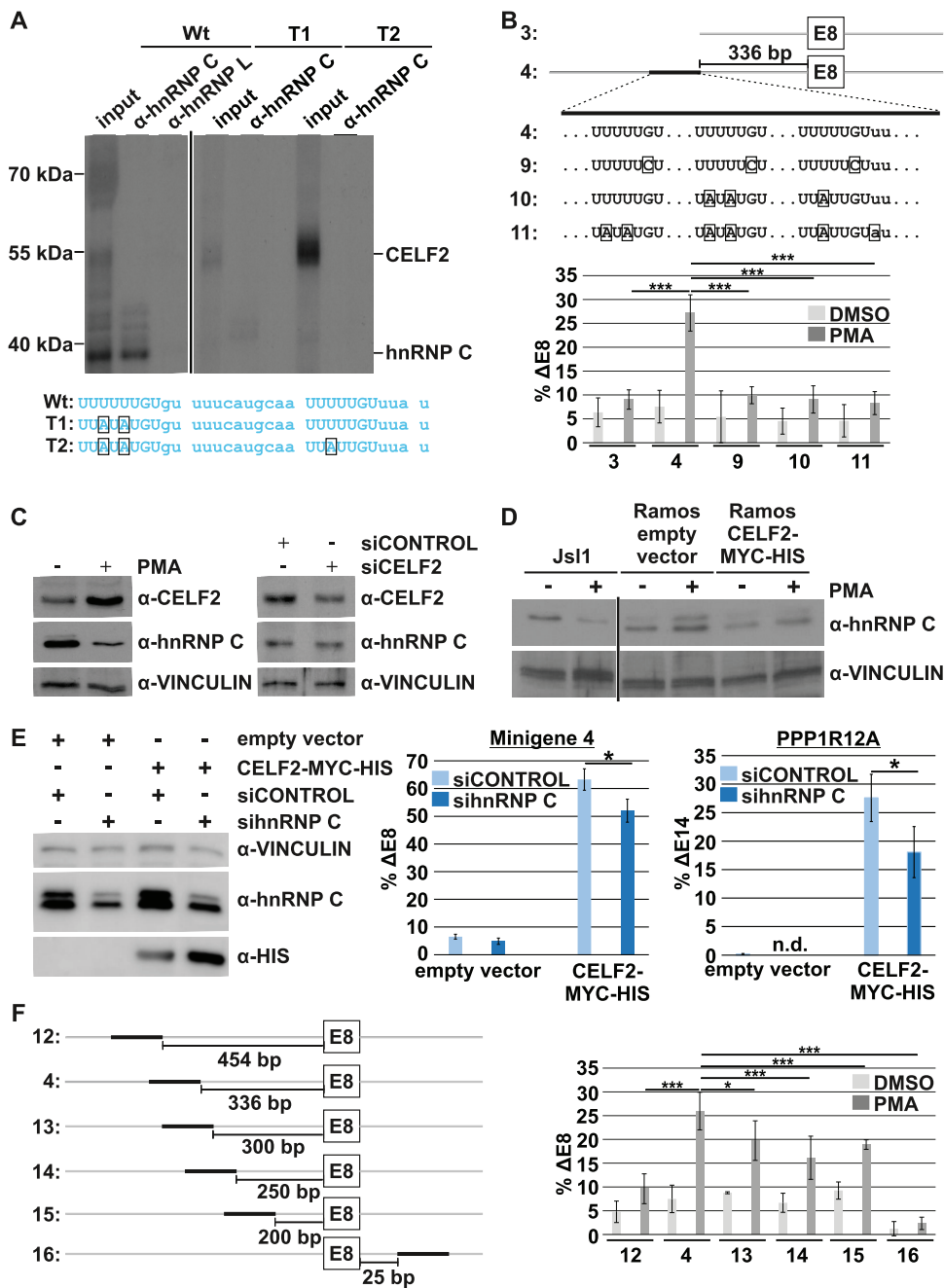


**FIG 6** hnRNP C and CELF2 binding to the *cis*-acting sequence and its distance to the exon control splicing regulation. (A) Part 3 of the TRAF3 wild-type *cis*-acting element or sequences with U-to-A mutations (at the bottom of the panel, nucleotide changes are indicated by boxes) were radioactively labeled, and cross-link IPs with extracts from unstimulated Jsl1 cells were performed with hnRNP C or the control hnRNP L antibody. A representative autoradiography from three independent experiments is shown. (B) Splicing of minigenes with mutations corresponding to the point mutants shown in Fig. 5C was analyzed as in Fig. 1B. Mutations in construct 9 prevent CELF2 binding, and those in constructs 10 and 11 prevent hnRNP C binding. A scheme and the sequences used are shown at the top; mean values for percent TRAF3 exon 8 exclusion in DMSO- and PMA-treated cells from at least three independent experiments are shown below (\*\*\*,  $P < 0.001$ ). (C) Western blot showing hnRNP C and CELF2 expression in unstimulated (–) or stimulated (+) T cells and cells with CELF2 knockdown. Vinculin served as a loading control. (D) Western blot comparing hnRNP C expression in different cell types and conditions, as indicated. (E) HEK293 cells were transfected as indicated and also with the TRAF3 minigene 4. A Western blot (left) confirms hnRNP C knockdown and CELF2 overexpression with vinculin as a loading control. TRAF3 minigene splicing (middle) or PPP1R12A endogenous splicing (right) under different conditions was analyzed as in panel B. Mean values of three independent experiments are shown. n.d., not detected. (F) Minigenes in which the distance of the ISS to the exon was altered as indicated (left) were transfected in Jsl1 T cells, and splicing was analyzed as in panel B (right). Mean values of at least three independent experiments are shown (\*,  $P < 0.05$ ; \*\*\*,  $P < 0.001$ ).

the involvement of both proteins in TRAF3 exon 8 alternative splicing. Furthermore, hnRNP C knockdown had no effect on TRAF3 exon 8 skipping in the absence of CELF2, supporting a model in which hnRNP C is necessary for CELF2-mediated exon skipping but has little effect on its own. The same effect was observed for PPP1R12A alternative splicing, which was affected by hnRNP C knockdown only in the presence of CELF2 (Fig. 6E), suggesting the interplay between the two proteins to be of broader significance for splicing regulation.

The intronic splicing silencer that controls activation-induced TRAF3 exon 8 skipping shows some interesting features: its location is more than 300 nt upstream of the regulated exon, and it is strictly dependent on two *trans*-acting factors, which are antagonistically regulated upon T cell activation. As a first step toward understanding the mode of splicing regulation of this unusual *cis*-acting element, we analyzed its dependence on the location relative to the regulated exon. Interestingly, moving the ISS approximately 100 nt further away from the exon completely abolished its activity (Fig. 6F, minigene 12). Moving the ISS within the upstream intron to positions closer to the exon, i.e., 300, 250, or 200 nt upstream of the 3' splice site (minigenes 13 to 15), did significantly reduce splicing regulation upon PMA stimulation, whereas inserting the sequence in the downstream intron abolished the effect completely (Fig. 6F, minigene 16). These data show that full activity of the ISS is dependent on its precise location upstream of the regulated exon.

## DISCUSSION

Regulatory elements that control cell-type-specific alternative splicing remain largely unknown. Here we define a *cis*-acting RNA sequence in the TRAF3 transcript (Fig. 1), as well as the *trans*-acting factors, CELF2 and hnRNP C, that bind to this sequence, in order to induce skipping of TRAF3 exon 8 upon T cell activation (Fig. 2 to 6). We used a conventional minigene approach to identify *cis*-acting elements and combined UV cross-link IPs with a targeted siRNA screen to identify the *trans*-acting factor. Knockdown screens can be performed without identifying the *cis*-acting elements first (36–38), and splicing of the endogenous gene can be used as readout, thus providing an interesting alternative to the classical RNA-protein interaction-based approaches often used following minigene analyses to identify *trans*-acting factors.

Since the expression of CELF2 is induced upon activation of T cells but not in other cell types, such as B cells (Fig. 4), our data suggest a prominent role for CELF2 expression in controlling activation-induced alternative splicing in a manner that depends on the cellular background. The effect of CELF2 expression on alternative splicing of TRAF3 exon 8 appears to be independent of the cellular context, since it happens in various cell types (Fig. 4). Since the expression of endogenous CELF2 is not limited to activated T cells (26, 27), regulated CELF2 expression may be sufficient to control alternative splicing of several or many targets during development and differentiation. This idea is consistent with the recent finding that overexpressing human CELF2 in mouse heart leads to substantial changes in the global splicing pattern; among the potential target exons found in this study was TRAF3 exon 8, which was not found when overexpressing CELF1 (28). It should be noted, however, that there is only little overlap between the exons regulated by CELF2 overexpression in the heart and CELF2 knockdown in T cells (28, 30), which may indicate a tissue-specific regulation of CELF2 activity. One possibility is alternative splicing of CELF2 itself (27, 39), which, based on reference sequences, gives rise to many different isoforms. In our analysis, we tested two human CELF2 isoforms, RefSeq [NM\\_001025076.2](#) (isoform 1) and [NM\\_001083591.1](#) (isoform 4) without observing differential activities with respect to TRAF3 exon 8 skipping (Fig. 4F). In addition, we identified hnRNP C to be essential for CELF2-mediated TRAF3 exon 8 skipping, since mutations that abolish either hnRNP C or CELF2 binding both render minigenes unresponsive to PMA stimulation. We thus consider it very likely that CELF2 can exert different modes of splicing regulation; the one we identified here is dependent on hnRNP C, which targets different exons based on the sequence and location of the *cis*-acting elements. hnRNP C was recently identified to bind another

CEL2 target exon, namely, an exon within MKK7 (35). HnRNP C appeared not to be sufficient for splicing regulation of this exon, but it would be interesting to further analyze whether it might be necessary for CEL2-mediated splicing control since this would indicate a more general role of this mechanism. A recent report has suggested that the location of CEL2 binding upstream or downstream of the exon determines the outcome of splicing regulation, exclusion or inclusion, respectively (40). For this model, CEL2 binding was analyzed up to a distance of 300 nt upstream or downstream of the exon, and the top binding motif based on CLIP tags did not include the oligo(U) stretch, which we found to be required for hnRNP C binding (40). These differences may explain the different outcome of CEL2 binding compared to our study, where the distance and cobinding of hnRNP C determine the activity of the intronic element, and together point to different modes of CEL2-mediated exon repression. Different modes of splicing regulation, dependent on the sequence and location of *cis*-acting elements and the expression and binding of additional *trans*-acting factors, would allow a complex regulation of tissue-specific alternative splicing and could explain different behaviors of CEL2 target exons in different cell types.

Another interesting aspect of our work is the location of the intronic splicing silencer sequence between 340 and 440 nt upstream of the regulated TRAF3 exon 8 (Fig. 1). This distance is larger than in most known cases, since many current analyses have focused on the 300 nt flanking the regulated exon (41, 42). Our data suggest that *cis*-regulatory sequences can be located further away from the target exon, and more such examples may be discovered in future analyses. Intronic splicing regulatory elements that are several kilobases away from the regulated exon have been reported. In these cases, *trans*-acting factors bound to the intronic *cis* elements are positioned in the vicinity of the exon through long range RNA-RNA base pairing (43). In analogy, hnRNP C, which has been shown to be able to form a tetramer and wind up RNA of around 240 nt (44, 45), could induce formation of a higher-order structure that places CEL2 in the vicinity of the regulated exon in order to control splicing. If the *cis*-acting sequence is moved closer to or further away from the exon, hnRNP C could still wind up RNA, but this could result in suboptimal positioning of the CEL2 relative to the exon and a reduced effect on splicing. However, this hypothesis is speculative at the moment, and further work is required to characterize the precise mechanism of exon skipping mediated by CEL2 and hnRNP C bound to an intronic sequence upstream of the regulated exon.

We identified a G residue surrounded by U residues that is crucial for CEL2 binding and full activation-induced exon skipping (Fig. 5). This observation fits well with previous studies, since CEL2 is known to bind GU-rich RNAs and in a Selex approach all enriched 5mers and 6mers contained a UGU sequence (46). However, the *cis*-acting element that we have identified here contains an additional oligo(U) stretch, which serves as hnRNP C binding site and is essential for splicing regulation. Interestingly, the intron upstream of the alternative PPP1R12A exon that strongly responded to CEL2 expression contains two UUUUGU motifs 340 and 380 nt upstream of the 3' splice site. This distance perfectly matches the distance observed for TRAF3 exon 8. Other exons, for example in BRD8, FAM36 or REPS1, responded less strongly to CEL2 overexpression. Within 1 kb of the upstream intronic sequence, these less-responsive exons contain one or two UUUUGU motifs, 100 nt (Brd8), 930 nt (Fam36A), or 120 and 810 nt (REPS1) upstream of the exon. The reduced response to CEL2 overexpression suggests either a different mode of splicing regulation or a weaker effect due to the suboptimal distance of the *cis*-regulatory sequence to the exon, again pointing to an impact of the location of the *cis*-acting element on the responsiveness of an exon. Whether this is further controlled by the relative CEL2 and hnRNP C binding strength and thus a ratio of both proteins on the pre-mRNA is a question that remains to be addressed. Similarly, whether CEL2 and hnRNP C bind in a cooperative or antagonistic manner (our data pointing to the latter as CEL2 binding is slightly increased in the mutants that do not bind hnRNP C anymore) or bind completely independent from one another is another question to be addressed in order to understand the mechanism of splicing control of this unusual intronic element.

Altogether, we have identified the *cis*- and *trans*-acting components that regulate TRAF3 exon 8 skipping, a functionally important splicing switch during T cell activation. Our data suggest that additional exons are regulated in a concerted manner, thus pointing to a CELF2- and hnRNP C-dependent mechanism that controls activation-induced alternative splicing in a manner that depends on the CELF2 expression level. This is mediated through a distance-dependent intronic splicing silencer that is located >300 nt upstream of the regulated exon. Based on our work, future studies will likely uncover more such elements and show whether distantly localized intronic elements represent a common way of splicing regulation.

## MATERIALS AND METHODS

**Cell culture and transfections.** Jsl1, Raji, and Ramos cells were grown in RPMI medium containing 10% fetal bovine serum (FBS; Biochrom) and penicillin-streptomycin (Pen/Strep). HEK293 cells were cultivated in Dulbecco modified Eagle medium with the same additives. Both the media and the Pen/Strep were purchased from Biowest.

For the siRNA screen, transfection of siRNAs (10 pmol [siGenome SMARTpool; Dharmacon]) was performed using Amaxa Nucleofector according to the manufacturer's protocol for Jurkat cells, except that instead of Nucleofector solution, RPMI medium without additives was used. siRNA transfections for validations were performed using HiPerfect (Qiagen) with 20 pmol of ON-TARGETplus SMARTpool (Dharmacon) or individual siRNAs according to the manufacturer's instructions. One day after transfection cells were treated with PMA or dimethyl sulfoxide (DMSO) for 48 h.

Minigene transfections were done as described previously (18). Briefly,  $10^7$  cells were harvested, washed with RPMI medium without additives, and then transferred into an electroporation cuvette containing 5 to 10  $\mu$ g of plasmid. Electroporation was performed at 250 mV and 960  $\mu$ F. Transfected cells were cultured in RPMI medium with additives. One day after transfection, cells were treated with PMA (Sigma; final concentration, 20 ng/ $\mu$ l) or solvent control (DMSO) for 48 h and then harvested. For the minigene assays (Fig. 6), the extracted RNAs were treated with DNase prior to the RT reaction.

To establish a Ramos cell line which stably overexpresses CELF2, the CELF2-MYC-HIS plasmid was linearized, and transfection was performed by electroporation as described above. Positive clones were selected with G418 (Sigma) at 4 mg/ml in RPMI medium containing 10% FBS.

HEK293 cells were transfected using RotiFect (Carl Roth) as described in the manual, and the cells were harvested at 48 h posttransfection.

**RNA, RT-PCR, and qRT-PCR.** RNA extraction, reverse transcription-PCR (RT-PCR), phosphorimager quantification, and reverse transcription-quantitative PCR (RT-qPCR) were all performed as previously described (31, 47). The percent PMA-induced exon skipping was defined as % inclusion without PMA treatment – % inclusion with PMA stimulation. Quantification of gene expression represents mean values of at least three independent experiments (exact numbers are given in the figure legends), and error bars represent the standard deviations. Significance was calculated by using a Student unpaired *t* test (\*,  $P < 0.05$ ; \*\*,  $P < 0.01$ ; \*\*\*,  $P < 0.001$ ). Primer sequences are provided in the supplemental material.

**Western blotting and UV cross-linking.** Protein extraction was performed in standard lysis buffer (60 mM Tris [pH 7.5], 30 mM NaCl, 1 mM EDTA, 1% Triton X-100). SDS-PAGE and Western blotting were performed according to standard protocols. The antibodies used in Western blotting were as follows: anti-CELF2 (Sigma, catalog no. C9367), anti-GAPDH (anti-glyceraldehyde-3-phosphate dehydrogenase) (GeneTex, GT239), anti-hnRNP L (Santa Cruz, sc-32317), anti-hnRNP C (Santa Cruz, sc-32308), and antivinculin (Santa Cruz, sc-5573). Nuclear extracts were prepared as previously described (47).

UV cross-links were performed as described previously (33) with RNAs that were transcribed *in vitro* from linearized plasmid or annealed primers as the template in the presence of [ $\alpha$ - $^{32}$ P]UTP. For cross-link IPs, three samples were pooled after RNase digestion and incubated in 1 $\times$  radioimmunoprecipitation assay (RIPA) buffer (10 mM Tris [pH 8.0], 1% NP-40, 5 mg/ml sodium deoxycholate, 2 mM EDTA, and 100 mM NaCl containing protease inhibitors) and one of the following antibodies: anti-CELF1 (GeneTex, N1C1-2), anti-CELF2 (Sigma, C9367), anti-hnRNP C (Santa Cruz, sc-32308), and anti-hnRNP L (Santa Cruz, sc-32317) or anti-HA (Santa Cruz, sc-7392) as controls. The mixtures were rotated for 1 h at 4°C before 25  $\mu$ l of a prewashed 50% protein A-Sepharose bead suspension (Life Technologies) was added, and rotation was continued overnight. IPs were then extensively washed in 1 $\times$  RIPA buffer and analyzed by SDS-10% PAGE and autoradiography.

**Cloning.** The genomic TRAF3 region for minigene 1 was amplified by PCR from Jsl1 genomic DNA. Primers introduced restriction sites (NdeI and BamHI) to ligate the fragment into NdeI and BglII sites of a minigene vector containing constant CD45 exons flanking the TRAF3 sequence (CD background [33]). Shorter or mutated minigenes were cloned using existing minigenes as the template for PCR. The CELF2 coding region was PCR amplified from cDNA of stimulated Jsl1 cells introducing restriction sites for cloning. After digestion, the insert was ligated into SpeI/EcoRV-digested pEF1/myc-his B (Life Technologies). All constructs were verified by sequencing.

## SUPPLEMENTAL MATERIAL

Supplemental material for this article may be found at [https://doi.org/10.1128/ MCB.00488-16](https://doi.org/10.1128/MCB.00488-16).

**TEXT S1**, PDF file, 1.3 MB.

## ACKNOWLEDGMENTS

We thank members of the Heyd lab for constructive discussions and comments on the manuscript.

This study was funded by an Emmy-Noether fellowship of the Deutsche Forschungsgemeinschaft (He5398/3 to F.H.) and the Fritz Thyssen Foundation (Az. 10.12.1.158 to F.H. and R.K.).

## REFERENCES

- Nilsen TW, Graveley BR. 2010. Expansion of the eukaryotic proteome by alternative splicing. *Nature* 463:457–463. <https://doi.org/10.1038/nature08909>.
- Barbosa-Morais NL, Irimia M, Pan Q, Xiong HY, Guerousov S, Lee LJ, Slobodenic V, Kutter C, Watt S, Colak R, Kim T, Misquitta-Ali CM, Wilson MD, Kim PM, Odom DT, Frey BJ, Blencowe BJ. 2012. The evolutionary landscape of alternative splicing in vertebrate species. *Science* 338:1587–1593. <https://doi.org/10.1126/science.1230612>.
- Merkin J, Russell C, Chen P, Burge CB. 2012. Evolutionary dynamics of gene and isoform regulation in mammalian tissues. *Science* 338:1593–1599. <https://doi.org/10.1126/science.1228186>.
- Xu X, Yang D, Ding JH, Wang W, Chu PH, Dalton ND, Wang HY, Bermingham JR, Ye Z, Liu F, Rosenfeld MG, Manley JL, Ross J, Chen J, Xiao RP, Cheng H, Fu XD. 2005. ASF/SF2-regulated CaMKII $\delta$  alternative splicing temporally reprograms excitation-contraction coupling in cardiac muscle. *Cell* 120:59–72. <https://doi.org/10.1016/j.cell.2004.11.036>.
- David CJ, Chen M, Assanah M, Canoll P, Manley JL. 2010. HnRNP proteins controlled by c-Myc deregulate pyruvate kinase mRNA splicing in cancer. *Nature* 463:364–368. <https://doi.org/10.1038/nature08697>.
- Gabut M, Samavarchi-Tehrani P, Wang X, Slobodenic V, O'Hanlon D, Sung HK, Alvarez M, Talukder S, Pan Q, Mazzoni EO, Nedelec S, Wichterle H, Woltjen K, Hughes TR, Zandstra PW, Nagy A, Wrana JL, Blencowe BJ. 2011. An alternative splicing switch regulates embryonic stem cell pluripotency and reprogramming. *Cell* 147:132–146. <https://doi.org/10.1016/j.cell.2011.08.023>.
- Wilhelmi I, Kanski R, Neumann A, Herdt O, Hoff F, Jacob R, Preußner M, Heyd F. 2016. Sec16 alternative splicing dynamically controls COPII transport efficiency. *Nat Commun* 7:12347. <https://doi.org/10.1038/ncomms12347>.
- Yang X, Coulombe-Huntington J, Kang S, Sheynkman GM, Hao T, Richardson A, Sun S, Yang F, Shen YA, Murray RR, Spirohn K, Begg BE, Duran-Frigola M, MacWilliams A, Pevzner SJ, Zhong Q, Trigg SA, Tam S, Ghamsari L, Sahni N, Yi S, Rodriguez MD, Balcha D, Tan G, Costanzo M, Andrews B, Boone C, Zhou XJ, Salehi-Ashtiani K, Charleatoux B, Chen AA, Calderwood MA, Aloy P, Roth FP, Hill DE, Iakoucheva LM, Xia Y, Vidal M. 2016. Widespread expansion of protein interaction capabilities by alternative splicing. *Cell* 164:805–817. <https://doi.org/10.1016/j.cell.2016.01.029>.
- Kalsotra A, Xiao X, Ward AJ, Castle JC, Johnson JM, Burge CB, Cooper TA. 2008. A postnatal switch of CELF and MBNL proteins reprograms alternative splicing in the developing heart. *Proc Natl Acad Sci U S A* 105:20333–20338. <https://doi.org/10.1073/pnas.0809045105>.
- Jensen KB, Dredge BK, Stefani G, Zhong R, Buckanovich RJ, Okano HJ, Yang YY, Darnell RB. 2000. Nova-1 regulates neuron-specific alternative splicing and is essential for neuronal viability. *Neuron* 25:359–371. [https://doi.org/10.1016/S0896-6273\(00\)80900-9](https://doi.org/10.1016/S0896-6273(00)80900-9).
- Boutz PL, Stoilov P, Li Q, Lin CH, Chawla G, Ostrow K, Shiue L, Ares M, Black DL. 2007. A posttranscriptional regulatory switch in polypyrimidine tract-binding proteins reprograms alternative splicing in developing neurons. *Genes Dev* 21:1636–1652. <https://doi.org/10.1101/gad.1558107>.
- Warzecha CC, Sato TK, Nabet B, Hogenesch JB, Carstens RP. 2009. ESRP1 and ESRP2 are epithelial cell-type-specific regulators of FGFR2 splicing. *Mol Cell* 33:591–601. <https://doi.org/10.1016/j.molcel.2009.01.025>.
- Heyd F, ten Dam G, Möryö T. 2006. Auxiliary splice factor U2AF26 and transcription factor Gfi1 cooperate directly in regulating CD45 alternative splicing. *Nat Immunol* 7:859–867. <https://doi.org/10.1038/ni1361>.
- Matlin AJ, Clark F, Smith CWJ. 2005. Understanding alternative splicing: towards a cellular code. *Nat Rev Mol Cell Biol* 6:386–398. <https://doi.org/10.1038/nrm1645>.
- Hertel KJ. 2008. Combinatorial control of exon recognition. *J Biol Chem* 283:1211–1215. <https://doi.org/10.1074/jbc.R700035200>.
- Heyd F, Lynch KW. 2009. Getting under the skin of alternative splicing: identification of epithelial-specific splicing factors. *Mol Cell* 33:674–676. <https://doi.org/10.1016/j.molcel.2009.03.001>.
- Topp JD, Jackson J, Melton AA, Lynch KW. 2008. A cell-based screen for splicing regulators identifies hnRNP LL as a distinct signal-induced repressor of CD45 variable exon 4. *RNA* 14:2038–2049. <https://doi.org/10.1261/rna.1212008>.
- Heyd F, Lynch KW. 2010. Phosphorylation-dependent regulation of PSF by GSK3 controls CD45 alternative splicing. *Mol Cell* 40:126–137. <https://doi.org/10.1016/j.molcel.2010.09.013>.
- Keshwani MM, Aubol BE, Fattat L, Ma C-T, Qiu J, Jennings PA, Fu X-D, Adams JA. 2015. Conserved proline-directed phosphorylation regulates SR protein conformation and splicing function. *Biochem J* 466:311–322. <https://doi.org/10.1042/BJ20141373>.
- Lipp JJ, Marvin MC, Shokat KM, Guthrie C. 2015. SR protein kinases promote splicing of nonconsensus introns. *Nat Struct Mol Biol* 22:611–617. <https://doi.org/10.1038/nsmb.3057>.
- Tan L-Y, Whitfield P, Llorian M, Monzon-Casanova E, Diaz-Munoz MD, Turner M, Smith CWJ. 2015. Generation of functionally distinct isoforms of PTBP3 by alternative splicing and translation initiation. *Nucleic Acids Res* 43:5586–5600. <https://doi.org/10.1093/nar/gkv429>.
- Ule J, Ule A, Spencer J, Williams A, Hu J-S, Cline M, Wang H, Clark T, Fraser C, Ruggiu M, Zeeberg BR, Kane D, Weinstein JN, Blume J, Darnell RB. 2005. Nova regulates brain-specific splicing to shape the synapse. *Nat Genet* 37:844–852. <https://doi.org/10.1038/ng1610>.
- Warzecha CC, Shen S, Xing Y, Carstens RP. 2009. The epithelial splicing factors ESRP1 and ESRP2 positively and negatively regulate diverse types of alternative splicing events. *RNA Biol* 6:546–562. <https://doi.org/10.4161/rna.6.5.9606>.
- Li Q, Zheng S, Han A, Lin C-H, Stoilov P, Fu X-D, Black DL. 2014. The splicing regulator PTBP2 controls a program of embryonic splicing required for neuronal maturation. *eLife* 3:e01201. <https://doi.org/10.7554/eLife.01201>.
- Venables JP, Brosseau JP, Gadea G, Klinck R, Prinos P, Beaulieu JF, Lapointe E, Durand M, Thibault P, Tremblay K, Rousset F, Tazi J, Abou Elela S, Chabot B. 2013. RBF2 is an important regulator of mesenchymal tissue-specific splicing in both normal and cancer tissues. *Mol Cell Biol* 33:396–405. <https://doi.org/10.1128/MCB.01174-12>.
- Ladd AN, Charlet BN, Cooper TA. 2001. The CELF family of RNA binding proteins is implicated in cell-specific and developmentally regulated alternative splicing. *Mol Cell Biol* 21:1285–1296. <https://doi.org/10.1128/MCB.21.4.1285-1296.2001>.
- Blech-Hermoni Y, Stillwagon SJ, Ladd AN. 2013. Diversity and conservation of CELF1 and CELF2 RNA and protein expression patterns during embryonic development. *Dev Dyn* 242:767–777. <https://doi.org/10.1002/dvdy.23959>.
- Wang ET, Ward AJ, Cherone JM, Giudice J, Wang TT, Treacy DJ, Lambert NJ, Freese P, Saxena T, Cooper TA, Burge CB. 2015. Antagonistic regulation of mRNA expression and splicing by CELF and MBNL proteins. *Genome Res* 25:858–871. <https://doi.org/10.1101/gr.184390.114>.
- Mallory MJ, Jackson J, Weber B, Chi A, Heyd F, Lynch KW. 2011. Signal- and development-dependent alternative splicing of LEF1 in T cells is controlled by CELF2. *Mol Cell Biol* 31:2184–2195. <https://doi.org/10.1128/MCB.05170-11>.
- Mallory MJ, Allon SJ, Qiu J, Gazzara MR, Tapescu I, Martinez NM, Fu X-D, Lynch KW. 2015. Induced transcription and stability of CELF2 mRNA drives widespread alternative splicing during T-cell signaling. *Proc Natl Acad Sci U S A* 112:E2139–E2148. <https://doi.org/10.1073/pnas.1423695112>.
- Michel M, Wilhelmi I, Schultz AS, Preussner M, Heyd F. 2014. Activation-induced tumor necrosis factor receptor-associated factor 3 (Traf3) alternative splicing controls the noncanonical nuclear factor  $\kappa$ B pathway and



- chemokine expression in human T cells. *J Biol Chem* 289:13651–13660. <https://doi.org/10.1074/jbc.M113.526269>.
32. Zarnack K, König J, Tajnik M, Martincorena I, Eustermann S, Stévant I, Reyes A, Anders S, Luscombe NM, Ule J. 2013. Direct competition between hnRNP C and U2AF65 protects the transcriptome from the exonization of Alu elements. *Cell* 152:453–466. <https://doi.org/10.1016/j.cell.2012.12.023>.
  33. Motta-Mena LB, Heyd F, Lynch KW. 2010. Context-dependent regulatory mechanism of the splicing factor hnRNP L. *Mol Cell* 37:223–234. <https://doi.org/10.1016/j.molcel.2009.12.027>.
  34. Martinez NM, Pan Q, Cole BS, Yarosh CA, Babcock GA, Heyd F, Zhu W, Ajith S, Blencowe BJ, Lynch KW. 2012. Alternative splicing networks regulated by signaling in human T cells. *RNA* 18:1029–1040. <https://doi.org/10.1261/rna.032243.112>.
  35. Martinez NM, Agosto L, Qiu J, Mallory MJ, Gazzara MR, Barash Y, Fu X, Lynch KW. 2015. Widespread JNK-dependent alternative splicing induces a positive feedback loop through CELF2-mediated regulation of MKK7 during T-cell activation. *Genes Dev* 29:2054–2066. <https://doi.org/10.1101/gad.267245.115>.
  36. Oberdoerffer S. 2008. Regulation of CD45 alternative splicing by heterogeneous ribonucleoprotein, hnRNPL. *Science* 321:686–691. <https://doi.org/10.1126/science.1157610>.
  37. Meininger I, Griesbach RA, Hu D, Gehring T, Seeholzer T, Bertossi A, Kranich J, Oeckinghaus A, Eitelhuber AC, Greczmiel U, Gewies A, Schmidt-Supprian M, Ruland J, Brocker T, Heissmeyer V, Heyd F, Krappmann D. 2016. Alternative splicing of MALT1 controls signaling and activation of CD4<sup>+</sup> T cells. *Nat Commun* 7:11292. <https://doi.org/10.1038/ncomms11292>.
  38. Tejedor JR, Papasaikas P, Valcárcel J. 2015. Genome-wide identification of Fas/CD95 alternative splicing regulators reveals links with iron homeostasis. *Mol Cell* 57:23–38. <https://doi.org/10.1016/j.molcel.2014.10.029>.
  39. Suzuki H, Takeuchi M, Sugiyama A, Alam AK, Vu LT, Sekiyama Y, Dam HC, Ohki SY, Tsukahara T. 2012. Alternative splicing produces structural and functional changes in CUGBP2. *BMC Biochem* 13:1–12. <https://doi.org/10.1186/1471-2091-13-1>.
  40. Ajith S, Gazzara MR, Cole BS, Shankarling G, Martinez NM, Mallory MJ, Lynch KW. 2016. Position-dependent activity of CELF2 in the regulation of splicing and implications for signal-responsive regulation in T cells. *RNA Biol* 13:569–581. <https://doi.org/10.1080/15476286.2016.1176663>.
  41. Fu X-D, Ares M. 2014. Context-dependent control of alternative splicing by RNA-binding proteins. *Nat Rev Genet* 15:689–701. <https://doi.org/10.1038/nrg3778>.
  42. Xiong HY, Alipanahi B, Lee LJ, Bretschneider H, Merico D, Yuen RKC, Hua Y, Gueroussov S, Najafabadi HS, Hughes TR, Morris Q, Barash Y, Krainer AR, Jovic N, Scherer SW, Blencowe BJ, Frey BJ. 2015. The human splicing code reveals new insights into the genetic determinants of disease. *Science* 347:1254806. <https://doi.org/10.1126/science.1254806>.
  43. Lovci MT, Ghanem D, Marr H, Arnold J, Gee S, Parra M, Liang TY, Stark TJ, Gehman LT, Hoon S, Massirer KB, Pratt GA, Black DL, Gray JW, Conboy JG, Yeo GW. 2013. Rbfox proteins regulate alternative mRNA splicing through evolutionarily conserved RNA bridges. *Nat Struct Mol Biol* 20:1434–1442. <https://doi.org/10.1038/nsmb.2699>.
  44. Soltaninassab SR, McAfee JG, Shahied-Milam L, LeSturgeon WM. 1998. Oligonucleotide binding specificities of the hnRNP C protein tetramer. *Nucleic Acids Res* 26:3410–3417. <https://doi.org/10.1093/nar/26.14.3410>.
  45. Huang M, Rech JE, Northington SJ, Flicker PF, Mayeda A, Krainer AR, LeSturgeon WM. 1994. The C-protein tetramer binds 230 to 240 nucleotides of pre-mRNA and nucleates the assembly of 40S heterogeneous nuclear ribonucleoprotein particles. *Mol Cell Biol* 14:518–533. <https://doi.org/10.1128/MCB.14.1.518>.
  46. Faustino NA, Cooper TA. 2005. Identification of putative new splicing targets for ETR-3 using sequences identified by systematic evolution of ligands by exponential enrichment. *Mol Cell Biol* 25:879–887. <https://doi.org/10.1128/MCB.25.3.879-887.2005>.
  47. Preußner M, Wilhelmi I, Schultz A-S, Finkernagel F, Michel M, Möröy T, Heyd F. 2014. Rhythmic U2af26 alternative splicing controls PERIOD1 stability and the circadian clock in mice. *Mol Cell* 54:651–662. <https://doi.org/10.1016/j.molcel.2014.04.015>.